RESILIENT INFRASTRUCTURE
June 1–4, 2016
RESILIENT INFRASTRUCTURE LONDON 2016

EFFECTS OF NON-TRADITIONAL ISOLATOR PLACEMENT FOR SEISMIC RETROFIT

Adrian P. Crowder
McMaster University, Canada

Tracy C. Becker
McMaster University, Canada

ABSTRACT

Seismic isolation delivers improved performance by means of a flexible layer at which lateral deformation is concentrated. However, for seismic retrofit applications base isolation systems can be of considerable expense, in significant part because of major alterations required at the base of the structure. The cost of introducing an additional diaphragm, constructing a seismic gap, and modifying the foundation causes the initial cost of isolation to be significantly higher than traditional non-isolation retrofit methods. To minimize initial costs, isolators may be placed directly at the top of the column level, without an additional diaphragm, instead of at the base of the building. To investigate the effects of this placement and the limits of applicability, experiments were conducted at McMaster University of a column-bearing subassembly. These experiments tested bearings on increasing flexible steel columns, investigating the effect of allowing end rotations on the bearing behaviour and the effect of large displacements on the overall stability of the beam-column system. This research looks at developing clear strength and stiffness requirements for the sub-isolation system with the aim of increasing the number of existing buildings that are candidates for retrofit with isolation.

Keywords: Seismic isolation; retrofit; experimental; substructure flexibility; rotation

1. INTRODUCTION

Seismic isolation is a method of earthquake resistant design which introduces a laterally flexible layer between a structure and the ground. During strong ground motions, the lateral deformations are concentrated at the isolation layer and the structure translates in near rigid body motion, limiting interstory drifts within the structure. Due to this highly flexible layer the natural period of the isolated structure is lengthened as well, and leads to lower accelerations within the structure. The methodology has been shown to significantly improve the response of structures during earthquake motions, and has seen exponential growth in its use after performing well during the 1995 Kobe earthquake (Clark, et al. 1999). Isolation systems have also been shown to provide excellent protection for non-structural components which typically account for a major portion of the value of commercial buildings (Kelly 1993). These highly desirable characteristics of isolated structures is recognized by the Federal Emergency Management Agency (FEMA) and has been recommended as an appropriate strategy for when enhanced performance objectives are required for a project (FEMA 1997).

Developments to the seismic design provisions in the National Building Code of Canada over the last 70 years have led to a significant portion of building stock to be inadequately designed for anticipated seismic events and require rehabilitation to ensure life-safety provisions are met (Caruso-Juliano, et al. 2014). Seismic isolation has been shown to be an effective strategy for retrofit projects (Matsagar and Jangid 2008), however, the strategy has proven to be expensive because of major alterations required at the base of the structure. Traditional isolation retrofit projects involve large excavation beneath the building, construction of an additional diaphragm, and construction of a seismic gap shown in Figure 1 (b). These key factors have caused previous isolation retrofit projects to be costly, with the isolators themselves only accounting for a small percentage of the total expenses (Kelly 1998).

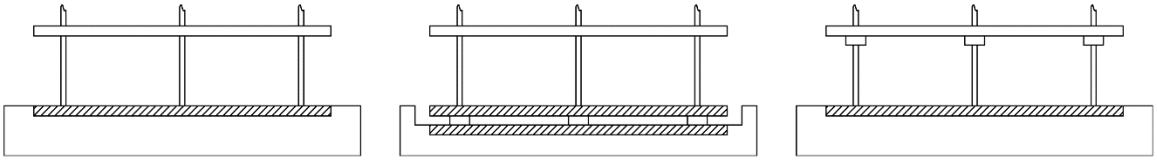

(a) (b) (c)

Figure 1: (a) pre-retrofit structure; (b) traditional isolation retrofit; (c) proposed isolation retrofit

To mitigate a large portion of the costs associated with isolation retrofit, it has been proposed to place the isolation layer on the tops of the first story columns, connecting the bearings between the column tops and the floor diaphragm above as shown in Figure 1 (c) (Matsagar and Jangid 2008). This installation method mitigates the need for a seismic gap, excavation beneath the building, and an additional rigid diaphragm. However, supporting columns must ensure adequate strength to remain elastic during extreme displacement demands in order to avoid soft story mechanisms. In addition, traditional installations typically require rigid diaphragms both above and below the isolation layer to distribute forces and maintain parallel end plates of the isolation bearings. Thus, understanding of the behaviour of isolation bearings has been developed assuming parallel end plates. In the proposed configuration, however, the bearings maintain a rigid connection with the floor diaphragm above but experience a flexible connection to the column below.

Despite most theories assuming parallel end plates, a handful of studies have considered the effects of end plate rotations on the behaviour of isolation bearings. Imbimbo and Kelly (1997) studied the effects of rotations on the stability of elastomeric isolators by extending the buckling theory proposed by Haringx (1949). By treating the bearing as a homogeneous column, the study considered a fixed-fixed configuration and a fixed-free configuration and concluded that a free end can reduce the buckling load by as much as half of the fixed-fixed configuration. Chang (2002) modelled the behaviour of individual rubber layers to obtain the global behaviour of an isolator under various loadings and boundary conditions. The study considered the impact of rigid versus free ends of isolation bearings and found that a free end will reduce the lateral stiffness. Karbakhsh Ravari et al (2012) approximated the global behaviour of a bearing and considered the effect of fixed amounts of rotation, showing that certain rotation can increase or decrease the lateral stiffness of isolation bearings. Crowder and Becker (2015) extended the theory to include uncoupled vertical deformations and developed a numerical model for use with OpenSees software (McKenna and Fenves 2006). Nonlinear time history analyses were conducted to compared the pre- and post-retrofit performance of a building designed using historical codes, and retrofitted with isolators on the tops of the first floor columns. The proposed isolation strategy showed effective reduction of interstory drifts and floor accelerations while stable performance of the bearings and columns was maintained.

To further study the behaviour of isolation bearings on flexible supports, cyclic quasi-static tests of column-bearing subassemblies were conducted at the Applied Dynamics Laboratory at McMaster University. Four columns with varying strength and stiffness were used to capture the effects of yielding and increased end-plate rotation. The results of the testing are presented and compared to determine the effects on end plate rotations, displacement distribution, lateral stiffness, and peak column moments. The results are used to draw conclusions concerning the usage of isolation systems with flexible end conditions and the demands on columns in a bearing-column subassembly.

2. EXPERIMENTAL PROGRAM

The experimental program was conducted at 1/4 scale and consisted of a square HSS in combination with an isolation bearing. The bearing was a circular natural rubber bearing manufactured to scaling requirements. The following are the pertinent dimensions: a diameter of 160 mm; 20 layers of 1.98 mm thick rubber for a total rubber thickness of 39.6 mm; 19 steel shims with 1 mm thickness; and a total bearing height of 101.8 mm. The shear modulus of the rubber was 0.4 MPa. The columns were selected so that the largest was not expected to experience yielding or significant rotation, while yielding and large rotations were expected to for the smallest. The following sections were selected, listed from least to most flexible: HSS127x127x8.0; HSS120x102x8.0; HSS76x76x4.8; and HSS64x64x4.8. All column specimens were 875 mm in length, and were welded to end plates which were bolted to the isolation bearing end plate. Stiffeners were added to the connections to ensure failure would not occur at the weld. The columns were outfitted with strain gauges on both sides along their height to determine bending moments and detect the formation of a plastic hinge.

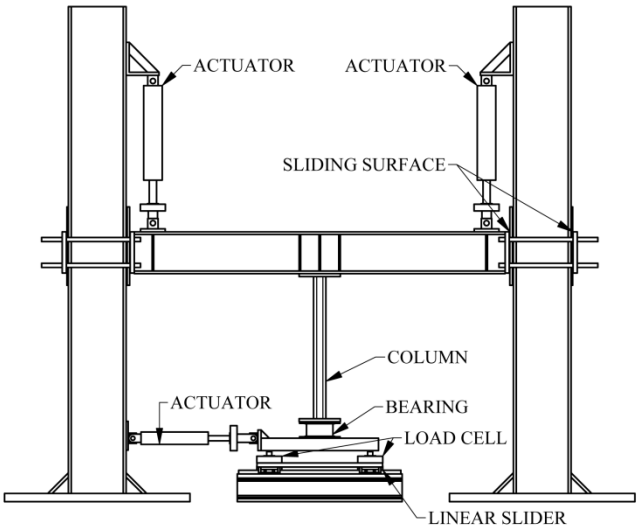

Figure 2: Setup designed for testing the column-bearing subassemblies

The test setup shown in Figure 2 was designed and constructed for testing the column-bearing subassemblies. Two vertical actuators provided a constant axial load. A loading beam wrapped around the reaction columns in order to provide out-of-plane support, and a low friction sliding surface was used between the loading beam and reaction columns to allow vertical movement with minimal force. A horizontal actuator drove a uniaxial table constructed on linear sliders with a displacement capacity of +/- 120 mm, providing the displacement control. Load cells located beneath the table provided reaction forces used to determine the axial and moment forces at the bottom of the isolation bearing. The setup was design to accommodate a variety of specimen heights and can be adjusted by raising or lowering the vertical actuators, loading beam, and sliding surfaces together along the reaction columns.

Tests of all four column-bearing subassemblies and of the bearing only were conducted using quasi-static cyclic testing at constant velocity. All tests were conducted with the same displacement time history to compare results and draw conclusions between systems with varying flexibilities. The displacement history provided multiple loops at +/- 10 mm, +/- 20 mm, +/- 40 mm, +/- 60 mm, +/- 80 mm, and +/- 100 mm cycles while a constant axial load was maintained to provide 6 MPa of pressure on the bearing. During testing of the most flexible column, the test was stopped at the completion of the +/- 80 mm cycles due to excessive rotations and a negative tangential stiffness in the system force-displacement hysteresis.

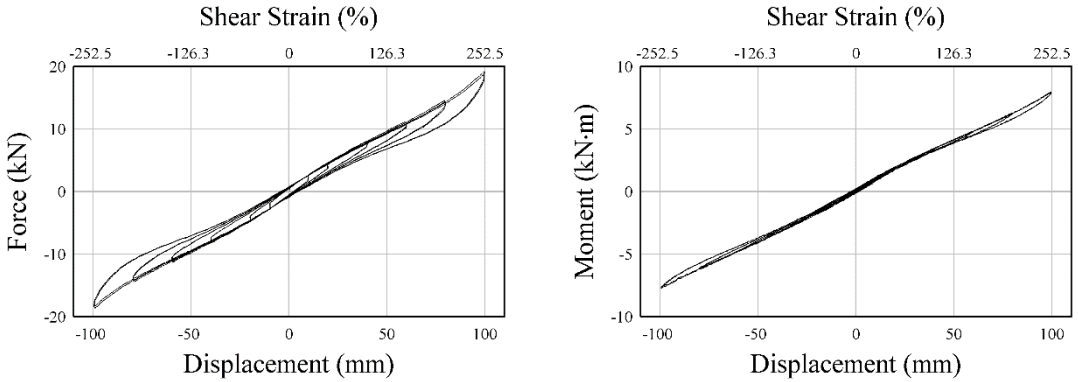

Figure 3: Force-displacement and moment-displacement of the bearing with parallel end plates

3. RESULTS

Preliminary testing was conducting with only the bearing installed in order to obtain the baseline behaviour of the isolator. The loading beam was lowered so the bearing could be bolted directly to the loading beam and the uniaxial

table, resulting in end plates remaining parallel during the test. The force-displacement and the moment-displacement behaviour are shown in Figure 3. The bending moments developed at the top of the bearing were found to be approximately linear with the displacement of the bearing. The force-displacement hysteresis of the bearing shows a slight hardening behaviour at large shear strains of approximately 200% which is typically a desirable behaviour in order to reduce displacements during extreme seismic events.

Following the bearing testing, the loading beam was repositioned to accommodate the column-bearing subassemblies. Testing of the least flexible column (HSS127x127x8.0) allowed small rotations to form at the bearing end plates causing a slight reduction in the deformations and forces as shown in Figure 4. The peak displacement of the bearing is slightly reduced compared to the bearing-only test due to a distribution of the displacement demand to both the bearing and the column. Due to the high stiffness of the column in the subassembly, the majority of displacement demand is concentrated in the isolation bearing and the reduction in displacement of the bearing is small. A hardening behaviour is still noted in the force-displacement hysteresis, but the effect is less pronounced because of lower shear strains achieved in the bearing. Rotations at the column-bearing interface were small due to the stiff connecting column, but show an approximately linear relationship with the shear force and bending moment at the bearing column interface. The existence of the rotations indicate the partial releasing of the fixity at the bearing end plate, and causes the moment to decrease at the bearing top plate when compared with the rigid testing in Figure 3. The column remained elastic for the duration of the test due to both its high moment resistance and the limited displacement demand experienced because of its high stiffness. As more flexible columns were tested, displacement demands on the isolator, shear forces and bending moments all decreased, while rotations at the column-bearing interface and the column displacements continued to increase.

Testing of the most flexible column (HSS64x64x4.8) showed a significant displacement distribution to the column and yielding occurred at the end furthest from the bearing during the largest displacement cycles. As the bearing experienced smaller displacement demands with increasingly flexible columns, the hardening behaviour in the bearing force-displacement hysteresis was no longer achieved. The bearing began to undergo nonlinear behaviour as shown in Figure 5, and peak rotations in excess of 2.5 degrees at the column-bearing interface were recorded.

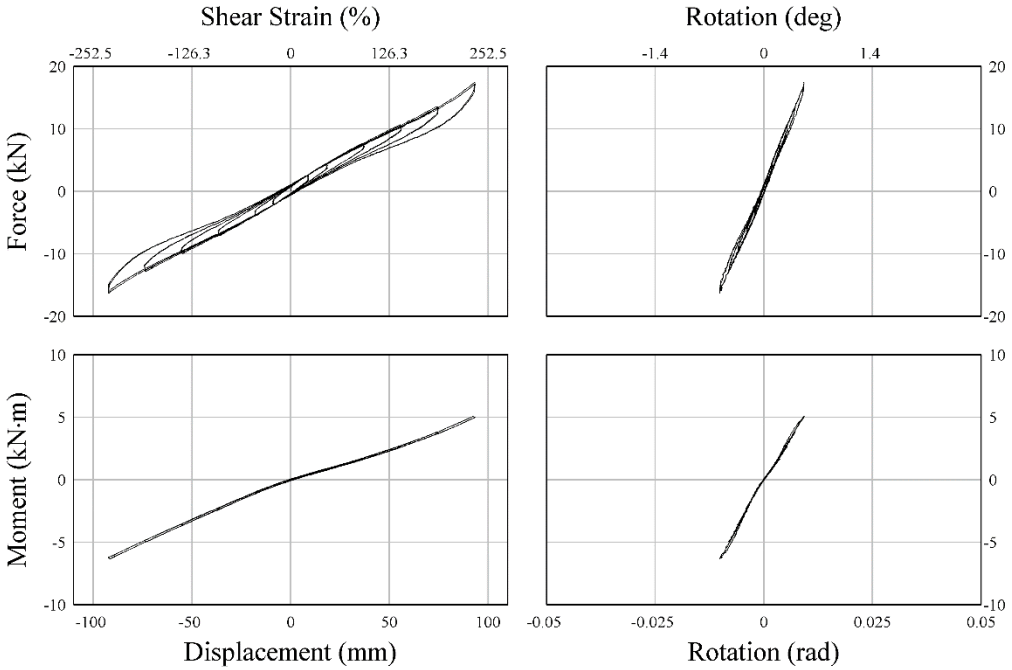

Figure 4: Bearing response in the HSS127x127x8.0 subassembly

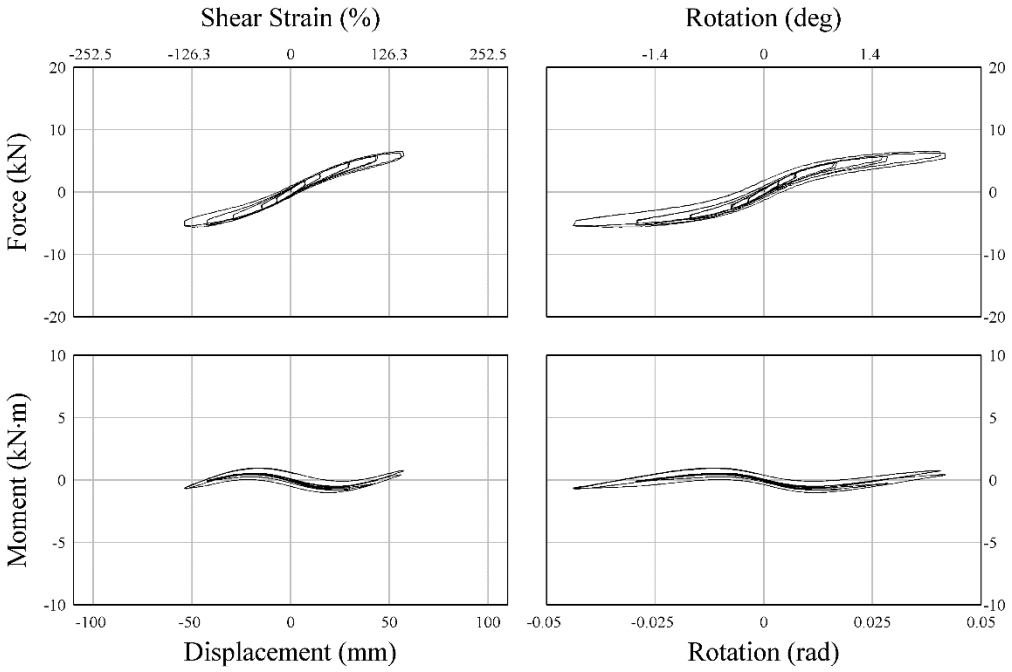

Figure 5: Bearing response in the HSS64x64x4.8 subassembly

A notable difference between the most flexible column (Figure 5) with the stiff column/rigid boundary condition (Figures 3 and 4) is the change in sign of the initial stiffness in the moment-displacement and moment-rotation relationships. This change in sign for the moment relationships can be understood by considering the moments developed for translation and rotation of the bearing, shown in Figure 6. As the bearing deforms in positive displacement with rotation fixed, a positive moment is required for equilibrium; as the bearing deforms in positive rotation with translation fixed, a negative moment reaction develops. For stiff column subassemblies the rotation of the bearing top plate remains small while translation is large, resulting in positive moments. As the column becomes flexible, rotations increase while bearing translations decrease and the moments become negative. As a result of these interactions, when translation governs the bearing undergoes double curvature and the inflection point is located in the bearing, while when rotation governs the bearing is in single curvature and the inflection point moves outside of the bearing into the column. The latter case can be seen experimentally in Figure 7 with the most flexible column, where the rotation governed and the bearing was in single curvature.

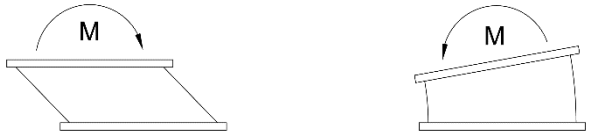

Figure 6: (a) positive displacement resulting in positive moment and double curvature; (b) positive rotation resulting in negative moment and single curvature


Figure 7: Large positive rotation of the bearing in the HSS64x64x4.8 subassembly resulting in single curvature

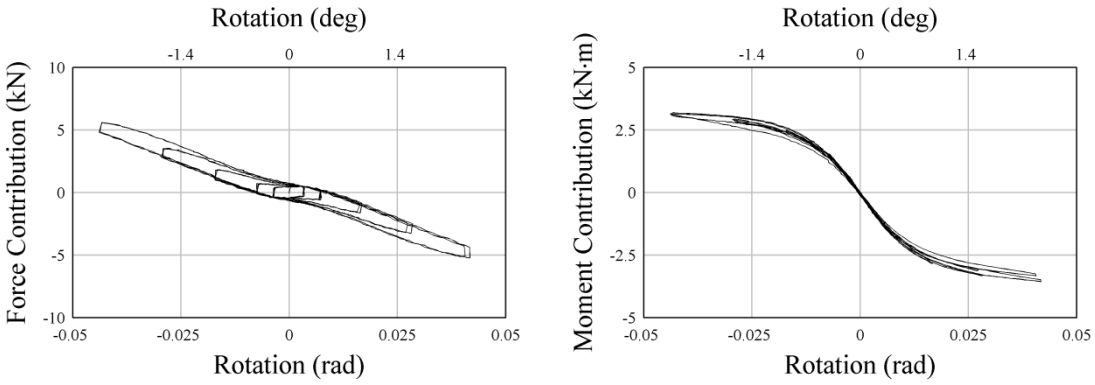

Figure 8: Force and moment components caused by rotation in the HSS64x64x4.8 subassembly

The nonlinear behaviour in the moment relationships in Figure 5 are likely associated with softening of the moment-rotation relationship described in Figure 6 (b). If the bearing behaviour is represented by a stiffness matrix as shown in Equation 1, the force and moment can be separated into components caused by translation and by rotation.

$$[1] \qquad \begin{bmatrix} V \\ M \end{bmatrix} = \begin{bmatrix} k_{11} & k_{12} \\ k_{21} & k_{22} \end{bmatrix} \begin{bmatrix} \Delta \\ \theta \end{bmatrix} = \begin{bmatrix} V_\Delta + V_\theta \\ M_\Delta + M_\theta \end{bmatrix}$$

From the preliminary testing of only the bearing in Figure 3, the rotations were zero and the resulting force and moments are solely caused by translation. Matching those results to the proposed stiffness matrix, the terms k_{11} and k_{21} are shown to be linear and can be determined from the experimental results. For the sake of modeling, if it is assumed that k_{11} and k_{21} are independent of the rotation, then the force and moment components caused by rotation can be determined by subtracting the translation components from the recorded total force and moment. Figure 8 presents the results of this subtraction and shows the force and moment components caused by rotation in the most flexible test. Both relationships are negative, and thus the total force and moment decrease when the bearing end plates are able to rotate. The force-rotation relationship is approximately linear, however, the moment-rotation relationship is seen to have a softening characteristic. The combination of the positive linear moment-translation relationship with the negative softening moment-rotation relationship results in the behaviour seen in Figure 5. At initial strains the moment response is negative and is governed by the moment-rotation relationship, but as softening occurs at higher strains the moment-translation relationship begins to govern and the response becomes positive.

The global force-displacement behaviour of the column-bearing subassembly of the stiffest and most flexible subassemblies is presented in Figure 9a. Figure 9b shows the force-displacement hystereses of the bearing for each of these test determined by subtracting out the column displacements. The comparison shows a reduction in stiffness between the stiffest to the most flexible column bearing subassembly, but this reduction is not solely due to the more flexible column. Figure 9b clearly shows a reduction in stiffness in the bearing as well. The decreased stiffness of

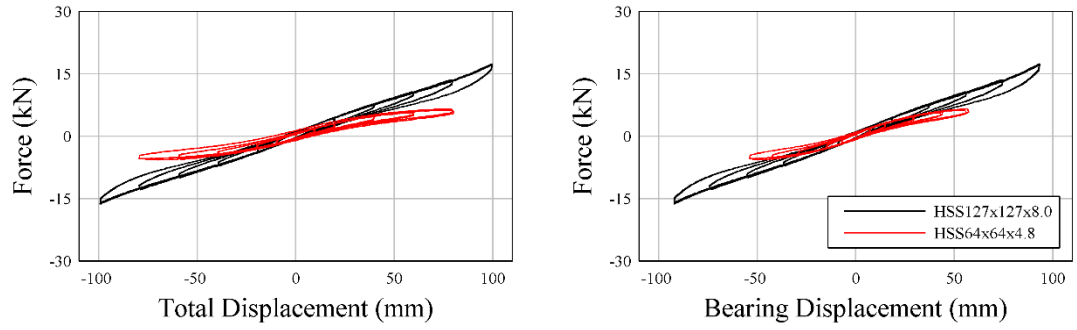

Figure 9: Change in force-displacement hystereses for (a) column-bearing subassembly; (b) bearing only

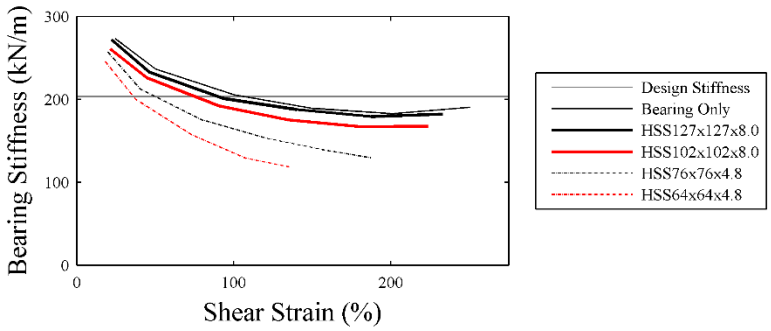

Figure 10: Bearing secant stiffness at varying displacement loops

the bearing is a direct result of the end conditions becoming more flexible and experiencing larger rotations, confirming previously theoretical studies (Change 2002, Ravari et al. 2012). Comparison of the hystereses also shows the differences in displacements experienced by the bearing versus the subassembly. For the stiffest column, the subassembly was cycled to +/- 100 mm with the bearing displacement of +/- 93 mm nearly equalling the full displacement. In contrast, the most flexible column was only cycled to +/- 80 mm but the bearing experienced a peak cyclic displacement of +/- 57 mm. The change in distribution of displacement to the bearing is largely a result of the changing column stiffness, however, as previously discussed there is also a contribution due to the changing stiffness of the bearing.

Figure 10 shows the secant stiffness of the bearing at each displacement cycle for each test specimen, along with the lateral stiffness traditionally used in the design process. The design lateral stiffness, representative of the lateral stiffness at 100% shear strain, compares well with the bearing-only test and the stiffest column. As more flexible columns are used, the lateral stiffness of the bearing decreases and diverges further from the design stiffness with increasing displacement. In the case of the most flexible column tested, the end plate rotations were large enough to reduce the lateral stiffness to as small as 58% of the design stiffness that would traditionally be assumed. For this reason, isolation systems with flexible connecting elements must account for the decrease in lateral stiffness in order to obtain reasonable estimates of the isolation period and peak displacements.

In order to estimate the amount of rotation experienced at the column-bearing interface, a relationship is desired to determine the rotation based on the displacement of the column. Due to the high rotational stiffness of the column in comparison to the bearing, the rotation at the column-bearing interface is governed by the column behaviour. A previous study by Crowder and Becker (2015) found that bending moment at the column-bearing interface tend to be negligible, allowing columns to be treated as fixed-free structures. Using traditional mechanics of a column and assuming fixed-free behaviour, the relationship in Equation 2 can be obtained to relate the column displacement to the bearing-column interface rotation.

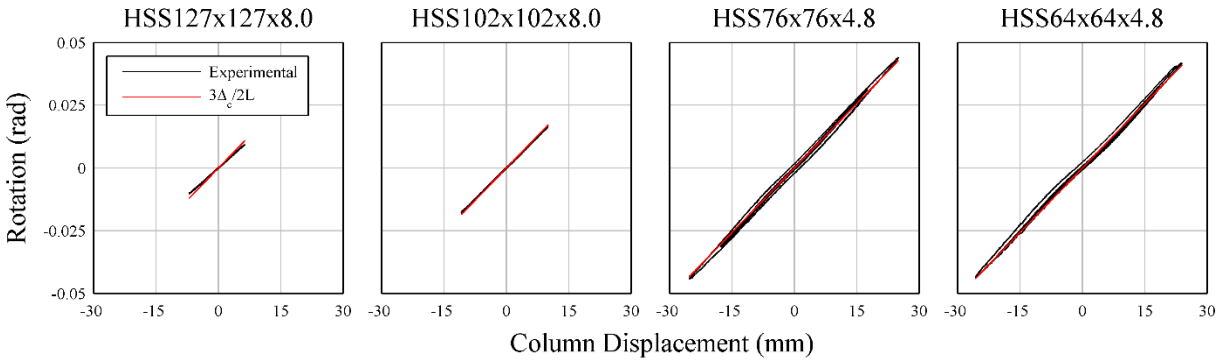

Figure 11: Relationship between the column displacement and the column-bearing interface rotation

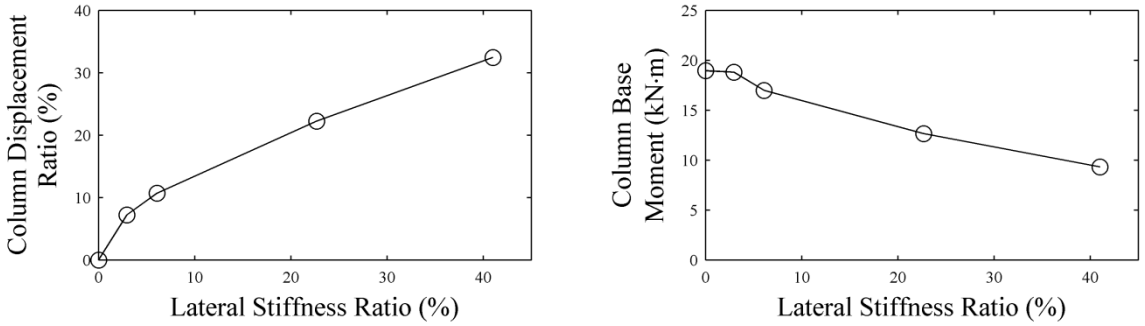

(a) (b)

Figure 12: Effect of stiffness ratio on (a) column displacement; (b) base moment

[2] $\theta = \frac{3\Delta_c}{2L}$

where Δ_c is the displacement of the column and L is the length of the column. Figure 11 shows the experimental relationship between the column displacement and the rotation at the column-bearing interface along with the relationship in Equation 2. The expression provides accurate prediction of the experimental results for most subassemblies tested. For the stiffest column the expression over-estimates the amount of rotation in the subassembly due to the existence of shear deformations. The depth to length ratio of the stiffest column (15%) cause shear deformations to contribute to displacement without increasing rotations, resulting in lower rotations than predicted by Equation 2.

By introducing a stiffness ratio (SR) in Equation 3, trends for the percentage of total displacement accommodated by the column and the peak moment in the column can be developed for a variety of subassemblies.

[3] $SR = \frac{K_b}{K_c}$

where K_b is the lateral stiffness of the bearing and K_c is the lateral stiffness of the column. A stiffness ratio of zero represents a rigid column while higher stiffness ratios represent more flexible columns in comparison to the bearing. Figure 12 shows the experimental results of the percentage of displacement distributed to the column and the peak base moment in the column as a function of the stiffness ratio. Since testing of the most flexible column was stopped at an earlier displacement cycle than all other tests, the results shown are the peak values reached at the +/- 80 mm cycles which was achieved by all tests. The base moment values at a stiffness ratio of zero were determined by assuming a rigid column of equal length to the tested columns, with simple mechanics of the end plate forces obtained from the bearing only test. The trends show increasing column displacement and decreasing base moment with increasing column flexibility.

4. CONCLUSIONS

This study considered the effects of placing the isolation layer, which is traditionally located at the base of a building, on the top of the first story columns. By placing the isolation layer in this configuration, bearings experience flexible connections to the columns resulting in the bearing end plates no longer remaining parallel. Experimental testing of column-bearing subassemblies were conducted at McMaster University's Applied Dynamics Laboratory to investigate the effects of column strength and stiffness on the sub-system. The investigation seeks to reduce the costs of isolation retrofit and extend the strategy to a more general class of structures, allowing more feasible and superior rehabilitation to Canada's current building stock. The results will also find applications in superstructure flexibility, isolation of bridge piers and tall buildings, and other scenarios where isolation bearings are susceptible to end plate rotations. The study concludes the following:

- The lateral stiffness of the bearing was reduced as end conditions became more flexible, verifying previously theoretical models.

- For stiff columns the response of bearings are approximately linear, but as column flexibility increases the bearing response becomes nonlinear due to a softening of the bearing moment-rotation relationship.
- Allowing larger end-plate rotation by increasing the flexibility of connecting elements results in a higher degradation of lateral stiffness with increasing shear strain and can lead to a significantly lower lateral stiffness than typically assumed.
- Rotations at the column-bearing interface are governed by the column and can be calculated using traditional mechanics based on the displacement of the column.

REFERENCES

Caruso-Juliano, A., Gallagher, A., Morrison, T. E. and Rogers, C. A. 2014. Seismic performance of single-storey steel concentrically braced frame structures constructed in the 1960s. *Canadian Journal of Civil Engineering*, 41 (7): 579-593.

Chang, C. 2002. Modelling of laminated rubber bearings using an analytical stiffness matrix. *International Journal of Solids and Structures*, 39 (24): 6055-6078.

Clark, P. W., Aiken, I. D., Nakashima, M., Miyazaki, M., and Midorikawa, M. 1999. *New Design Technologies*. Earthquake Engineering Research Institute.

Crowder, A. P., and Becker, T. C. 2015. Preliminary study on the behaviour of a column-top isolation system. *11th Canadian Conference on Earthquake Engineering*, Canadian Association for Earthquake Engineering, Victoria, British Columbia, Canada.

FEMA. 1997. *FEMA-273: Guidelines for the Seismic Rehabilitation of Buildings*. Federal Emergency Management Agency.

Haringx, J. A. 1949. *On highly compressible helical springs and rubber rods, and their application for vibration-free mountings, III*. Philips Research Reports 4.

Imbimbo, M., and Kelly, J. M. (1997). Stability Aspects of Elastomeric Isolators. *Earthquake Spectra*, 13 (3): 431-449.

Karbakhsh Ravari, A., Othman, I. B., Ibrahim, Z. B., and Ab-Malek, K. 2012. P-Δ and end rotation effects on the influence of mechanical properties of elastomeric isolation bearings. *Journal of Structural Engineering*, 138 (6): 669-675.

Kelly, J. M. 1993. *Earthquake Resistant Design with Rubber*. London: Springer- Verlag.

Kelly, J. M. 1998. Seismic isolation of civil buildings in the USA. *Progress in Structural Engineering and Materials*, 1 (3): 279-285.

Matsagar, V. A., and Jangid, R. S. 2008. Base isolation for seismic retrofitting of structures. *Practice Periodical on Structural Design and Construction*, 13 (4): 175-185.

McKenna, F., and Fenves, G. L. 2006. Open System for Earthquake Engineering Simulation (OpenSees). *Pacific Earthquake Engineering Research Center*. Retrieved from http://opensees.berkeley.edu/OpenSees/home/about.php